Analysis for coupling characteristics of optical microsphere cavity in waveguide coupled whispering gallery mode

WANG Meng-Yu[1]　　JIN Xue-Ying[1]　　LI Fei[1]　　ZHANG Yan-Chao[2]　　WANG Ke-Yi[1*]

(1. Department of Precision Machinery and Precision Instrumentation
University of Science and Technology of China　Hefei 230026　China;
2. Information Optoelectronics Research Institute　Harbin Institute of Technology　Weihai 264209　China)

Abstract：An efficient method for a coupled microsphere and waveguide system is proposed and demonstrated numerically and experimentally. In order to study the coupling characteristics of the microsphere-waveguide system　a two-dimensional (2D) model is exploited by the coupled theory firstly. A numerical simulation system is designed with the finite difference time domain (FDTD) method. The relative intensity spectra and transmission spectra in the wavelength range from 600 nm to 1000 nm are acquired by processing the sample data after fast fourier transformation (FFT). In the experiment　the quartz-microsphere is fabricated by melting the tip of a single-mode optical fiber. The tapered fiber　fabricated by using the heat-and-pull technique　is chosen as a waveguide to excite whispering gallery modes (WGMs) of the microsphere. The microsphere-taper coupling system is tested and the results indicate that a very high quality (Q) factor up to 2.3×10^6 and a high coupling efficiency up to 92.5% can be achieved by optimizing the microsphere position and orientation relative to the tapered fiber. These coupling characteristics can be well explained with the theoretical results. Such properties show its great potential in practical microcavity sensing and micro-lasers.

Key words：Micro-nano optics　microsphere resonator　waveguide optics　whispering gallery modes　FDTD　coupling characteristics
PACS：42. 70. Nq　42. 50. Pq　42. 81. Qb

　　　　　　　　　　　　　　　　　　1　　　　　*1*　　　　　*1*　　　　　*2*　　　　　*1**

　　　　　　　　　　　　(1.　　　　　　　　　　　　　　　　　　　　　　　　230026;
　　　　　　　　　2.　　　　　　　　　　　　　　　　　　　　264209)

　　　　　：　　　　　　　　　　　　　　　　　　　　　　　　　　　　　　　　　.

　　　　　　　　　　　　　　　　　　　　　2D　　.
　　　.　　　　　　　(FFT)　　　　　　　　　　　600 nm　　1 000 nm

　　　　　.　　　　　　　　　　　　　　　　　　　.

　　　　　　　　　　　　　　　　　　　−
　　　　　　　　　　　　2.3×10^6　　　　　92. 5% .

　　　.　　　　　　　　　　　　　　　　　　　　.
　　　　：　　　；　　　　　；　　　　；　　　　；　　　　　　；
　　　　：O43　　　　　　　：A

3

WANG Meng-Yu *et al*: Analysis for coupling characteristics of optical microsphere cavity in waveguide coupled whispering gallery mode

285

Introduction

In the past decade optical dielectric microcavities supporting whispering gallery modes (WGMs) have attracted considerable attention for a wide variety of fields such as nonlinear optics narrow linewidth micro-laser and high-sensitivity sensors. WGM microcavities have a variety of geometrical shapes including spheres disks toroids and even bubbles [1]. WGMs in them guide strongly light waves circulates about the equator of the cavity geometry by continuous total internal reflection (TIR) especially the microsphere ones leading to quality (Q) factors in excess of 10^8 being achieved. In addition to make light couple in and out of the microsphere a phase matched waveguide is essential to overlap the WGMs radiation field. Waveguide coupling using a tapered fiber with nearly ideal coupling efficiency is popularly considered in intensive studies [2]. The tapered fiber waveguide allows not only alignment and focusing of the input light but also collecting the output light. To analyze the microsphere-waveguide system the most commonly acknowledged numerical model is to use the FDTD method [3]. The method can precisely predict the electromagnetic (EM) field and the energy distributions. It is extremely effective to analyze these optimal systems associated WGM microcavities.

In this paper we present a general approach to describe coupling characteristics of WGM microsphere cavities coupled by a waveguide. A FDTD model of the microsphere-waveguide is described. Using the numerical methods the parameters for the microsphere size and the gap distance between the waveguide and microsphere can be selected. Ideal matching for a fiber waveguide to the WGMs of the microsphere is possible. The silica microspheres in the experiments are fused with the single mode fiber. The microsphere-taper system is tested featuring Q factor up to 10^6 and coupling efficiency up to 92.5%. The FDTD results present a good fit to our experimental results.

1 Theoretical results

The WGMs of axisymmetric microsphere cavities are EM resonances that belong to the wider family of Mie resonances and occur in a circular cavity [4]. As shown in Fig. 1 (a) the EM field of intra-microsphere when phase match can be approximated as two polarization modes (transverse magnetic (TM) or transverse electric (TE) polarization). To have a better understanding of the WGMs of microspheres we characterize the WGMs using four quantum indices (p q l m) p represents either TM or TE mode q represents the orders of the radical mode l represents the orders of the angular mode m represents the orders of the azimuthal mode. The fundamental mode ($q=1$ $l=m$) is usually more favorable conscious because it can realize higher photon degeneracy and smaller mode volume. WGM resonance inside the microsphere is typically a brilliant equatorial ring which is located on the same level with the waveguide. Thus it is suitable to utilize a 2D theoretical model to describe the course to excite WGMs as shown in

Fig. 1 (b).

(a)微球腔中的回音壁模式 (b)微球腔-波导耦合系统模型
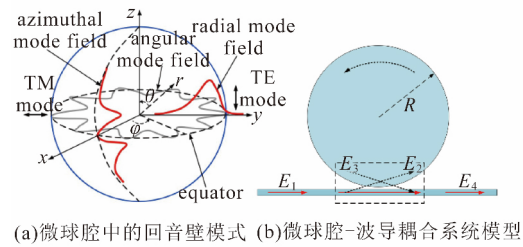
Fig. 1 Microsphere cavity model (a) the WGM mode of microsphere (b) model of microsphere-waveguide coupling system

To describe the behavior of the reflected beam quantitatively the optical field of the incident beam and the reflected beam can be regarded as E_1 and E_4 and the input beam and the output beam coupled in the microsphere can be regarded as E_2 and E_3. According to the coupled mode theory [5] the relationship of E_1 E_2 E_3 and E_4 can be speculated as:

$$\begin{bmatrix} E_2 \\ E_3 \end{bmatrix} = \begin{bmatrix} t & -k \\ k & t^* \end{bmatrix} \begin{bmatrix} E_1 \\ E_4 \end{bmatrix} \quad (1)$$

where $t(t = |t|* \exp(i\emptyset_t))$ is the field amplitude transmission coefficient through coupling system and $\emptyset_t$ is the phase mismatch factor and k is the resonator coupling parameter. E_3 will decrease to E_4 ($E_4 = \alpha \cdot \exp(i\theta) \cdot E_3$) affected by phase delay α and amplitude loss θ when it travels in the microsphere. The transmission power of the output port can be expressed as:

$$T = \left| \frac{E_4}{E_1} \right|^2 = \frac{\alpha^2 + |c|^2 - 2\alpha|c|\cos(\theta + \emptyset_t)}{1 + \alpha^2|c|^2 - 2\alpha|c|\cos(\theta + \emptyset_t)} \quad (2)$$

where phase mismatch factor $\emptyset_t$ can be negligible if coupling length of the silica microsphere-waveguide system is too short ($\emptyset_t$). When phase matches ($\Delta\beta = 0$ where $\Delta\beta$ stands for the transmission coefficient difference) coupling efficiency will reach the maximum the transmission E_4 of the output port can be represented in Fig. 2 (a). Based on the difference of the transmission curve E_4 the transmissions can be fell into three categories: under-coupled ($|t| > \alpha$) critically-coupled ($|t| = \alpha$) and over-coupled ($|t| < \alpha$) as showed in Fig. 2 (b). Most significantly critically-coupled filters all other waveguide modes efficiently save the fundamental mode at both the input and the output.

2 Numerical simulation model and analysis

WGMs can be interpreted as EM waves that circulate. Here we can simulate and calculate them by numerical computation. The FDTD method discretizes Maxwell's equation replacing derivatives with finite differences that are accurate to second order. Yee gird discretion form is applied in FDTD method. Figure 3 shows the
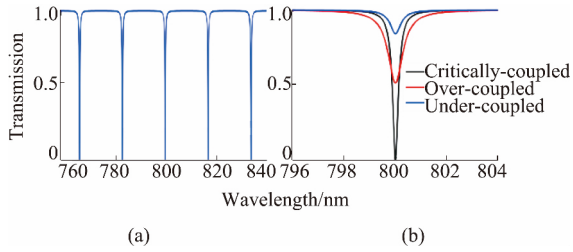
Fig. 2　Transmission of the coupling system（a）the trans-mission when phase matches（$\Delta\beta = 0$）（b）three typical transmissions（critically-coupled　over-coupled　and under-coupled）

2　　　　　　　　　　　　（a）　　　　　　　　　　　　（b）
　　　　　　　　　　　（　　　　　　　　　　　　　）

space position of grid cells and EM field components（E_x　E_y　E_z　H_x　H_y　H_z）in the right angle indicator system. We can see that there are four magnetic field components around each electric field component. EM components are arranged in cross limited by the basic conditions of Maxwell's equations. In the iteration process　these EM components sample in cross every other half time step. Each EM component factor keeps up-dating according to the former factor and the factors a-round them. When the medium is linear and isotropic the difference equations can be given as:

$$\begin{cases} \dfrac{\partial H_z}{\partial y} - \dfrac{\partial H_y}{\partial z} = \varepsilon \dfrac{\partial E_x}{\partial t} + \sigma_e E_x \\ \dfrac{\partial H_x}{\partial y} - \dfrac{\partial H_z}{\partial z} = \varepsilon \dfrac{\partial E_y}{\partial t} + \sigma_e E_y \\ \dfrac{\partial H_y}{\partial x} - \dfrac{\partial H_x}{\partial y} = \varepsilon \dfrac{\partial E_z}{\partial t} + \sigma_e E_z \end{cases} \quad (3)$$

$$\begin{cases} \dfrac{\partial E_z}{\partial y} - \dfrac{\partial E_y}{\partial z} = -\mu \dfrac{\partial H_x}{\partial t} - \sigma_m H_x \\ \dfrac{\partial E_x}{\partial y} - \dfrac{\partial E_z}{\partial z} = -\mu \dfrac{\partial H_y}{\partial t} - \sigma_m H_y \\ \dfrac{\partial E_y}{\partial x} - \dfrac{\partial E_x}{\partial y} = -\mu \dfrac{\partial H_z}{\partial t} - \sigma_m H_z \end{cases} \quad (4)$$

where ε　σ_e stand for the medium dielectric constant and conductivity　μ　σ_m represent the medium permeability and effective permeability.

In the cube grid　the grid size is $\Delta x = \Delta y = \Delta z = \Delta s$　the time step is Δt　we can get the EM filed factor of coordinate at $n\Delta t$ point if the time variable and the space variable is approximated by the second order differences operators. The time step need be set as $\Delta t = \Delta s/2c$ to ensure good numerical stability. Updated EM field com-ponents can be E_x^{n+1} and H_x^{n+1} can be written as:

$$E_x^{n+1}\left(i + \frac{1}{2}\ j\ k\right) = CA\left(i + \frac{1}{2}\ j\ k\right) \times E_x^n\left(i + \frac{1}{2}\ j\ k\right) + CB\left(i + \frac{1}{2}\right.$$

$$j\ k\right) \times \left[H_z^{n+\frac{1}{2}}\left(i + \frac{1}{2}\ j + \frac{1}{2}\ k\right) - H_z^{n+\frac{1}{2}}\left(i + \frac{1}{2}\ j - \frac{1}{2}\ k\right) + \right.$$

$$H_y^{n+\frac{1}{2}}\left(i + \frac{1}{2}\ j\ k - \frac{1}{2}\right) - H_y^{n+\frac{1}{2}}\left(i + \frac{1}{2}\ j\ k + \frac{1}{2}\right) \right] \quad (5)$$

$$H_x^{n+1}\left(i\ j + \frac{1}{2}\ k + \frac{1}{2}\right) = DA\left(i\ j + \frac{1}{2}\ k + \frac{1}{2}\right) \times H_x^{n-\frac{1}{2}}\left(i\ j + \frac{1}{2}\ k + \frac{1}{2}\right)$$

$$\left. \frac{1}{2}\right) + DB\left(i\ j + \frac{1}{2}\ k + \frac{1}{2}\right) \times \left[E_z^n\left(i\ j + \frac{1}{2}\ k + \frac{1}{2}\right) - \right.$$
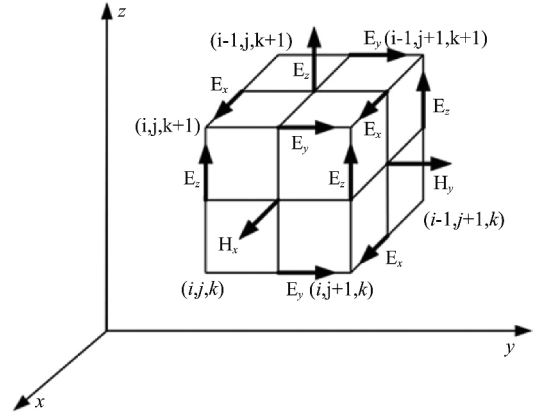
Fig. 3　Yee gird form in FDTD discretion
　　3　FDTD　　　　　　　　　Yee

$$E_y^n\left(i\ j + \frac{1}{2}\ k\right) + E_z^n\left(i\ j\ k + \frac{1}{2}\right) - E_y^n\left(i\ j + 1\ k + \frac{1}{2}\right) \right] \quad (6)$$

where $CA(i\ j\ k)$　$CB(i\ j\ k)$　$DA(i\ j\ k)$　$DB(i\ j\ k)$ are the coefficients.

We design a 2D FDTD numerical model based on a microsphere-waveguide coupling structure depicted in Fig. 4. The simulation domain adopted is normally a 13 μm × 13 μm rectangular area which is meshed 600 × 600 grids with the intention of ensuring the high computation-al accuracy. A well-known perfectly matched layer（PML）is chosen by absorbing boundary condition（ABC）to meet the calculated grid space in the condition of low reflection. A microsphere is positioned in the cen-tral model　and a wideband laser light beam is placed in the leftmost position of the waveguide and then couples to the resonator. When the wavelength of the incident light matches the natural resonance wavelength of the coupling system　WGM resonance happens. At the resonant wave-length　the relative intensity from the microsphere will rise rapidly and form a peak in the wavelength intensity spectra.

Specifically　the microsphere consists of silica glass and has a refractive index of $n_L = 1.46$. The waveguide is a single mode fiber with a width of d_w and a refractive index of $n_w = 1.46$. The surrounding medium is set to be air medium with $n_0 = 1$　but it can be any other medi-ums. The radius of the microsphere is R. The distance between the microsphere and the waveguide is g. A pulse mode source wave with cosine-modulated varies be-tween 600 nm and 1 000 nm　and the frequency varies 300 THz and 500 THz　correspondingly. For the sake of analyzing WGMs and resonance properties better　we place several sampling points in the position A　B　C and D as shown in Fig. 4. Location A and D describe the input field and the output field　and Location B and C stand for the microsphere field　respectively. The initial incident field for TM wave is employed in the leftmost boundary position. Main parameters are R　d_w　and g. Generally　the wider waveguide gets　the less the trans-mission loss. However　when the waveguide becomes too wide　this can cause multimode transmission easily which induces additional loss of energy. We can set: $d_w = 300$ nm. The effect of cavity loss must be noticed

3

WANG Meng-Yu *et al*: Analysis for coupling characteristics of optical microsphere cavity in
waveguide coupled whispering gallery mode

287
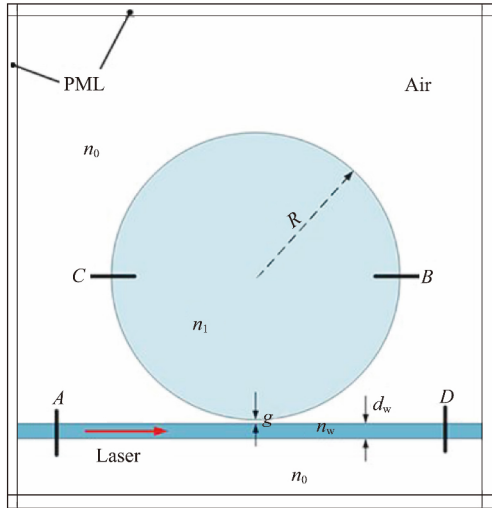
Fig. 4　FDTD simulation model of a microsphere
coupled to a waveguide
　　　4　　　　　　　　　　　　　FDTD

when to determine the microsphere size.

We record the data (W_1 and W_2) of the B and C
optical power for the first-order ($q = 1$)　second-order
($q = 2$)　and third-order ($q = 3$) resonance　the loss
factor can be obtained as: $c = (1 - W_1 / W_2)^2$. As the ra-
dius of the microsphere increases from $R = 2.5$ μm to R
$= 4$ μm　the cavity loss can be calculated as shown in
Fig. 5 (a) . It is found that the loss factor value of the
first-order resonance is the minimum and that of the
third-order is the maximum. The results illustrate that
loss factor will decrease rapidly when $R = 2.5$ μm increa-
ses to $R = 3$ μm　while it will rise slightly when $R = 3.25$
μm grows to $R = 4$ μm. Another reason is that bigger size
will subject to the larger memory requirement. Here　R
$= 3$ μm to $R = 3.25$ μm can be as experimental subjects
to obtain the lowest loss factor.

Coupling efficiency is a crucial reference when we
performed the FDTD simulations for the coupling system.
We find the gap strongly affects the coupling efficiency as
showed in Fig. 5 (b) . With an increasing distance of the
gap from 10 nm to 130 nm　the transmission curves of
the coupling system can be obtained in Fig. 6. The cou-
pling efficiency increases remarkably with a decrease of
the gap from 130 nm to 10 nm. The relative intensity
spectra can be got by processing the sample data (C) af-
ter FFT　as shown in Fig. 7. The blue　red　black
curves represent the resonance spectra of $R = 3$ μm　$R =$
3.125 μm　and $R = 3.25$ μm　respectively. It is found
that the resonance shift with the change of R. We ob-
tained the best parameters: $d_w = 300$ nm　$R = 3.25$ μm
$g = 10$ nm. Furthermore　FWHM grows wider with the
increasing wavelength. It may be a consequence of the
larger overlap of the waveguide field and WGMs field. It
is well-known that the evanescent light wave penetrating
in the surrounding medium is directly proportional to the
wavelength. Consequently　the depth of the evanescent
field will increase due to the increase of the wavelength
leading to a larger mode overlap. That will bring about a

(a)

(b)
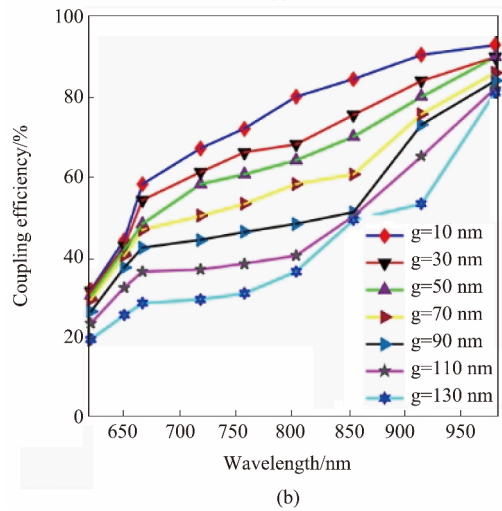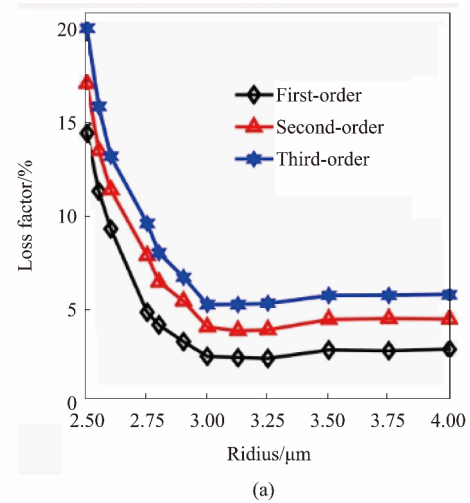
Fig. 5　Loss factor and coupling efficiency of the
coupling system (a) loss factor as a function of the
radius of microsphere R　(b) coupling efficiency as a
function of the incident wavelength λ_0 with different g
　　　5　　　　　　　　　　　　　　　(a)
　　　　　　　　　　　　(b)
　　　　　　　　　g
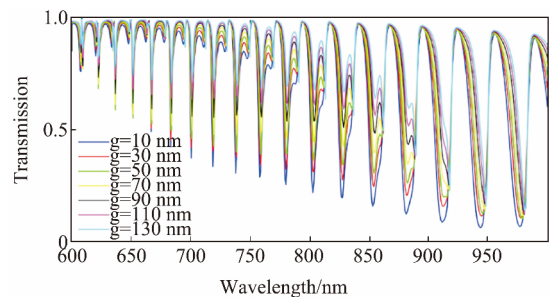
Fig. 6　Transmission of the coupling system
　　　6

larger coupling loss　which increases the FWHM.

3　Experimental results

In the experiment　the silica microspheres are fabri-
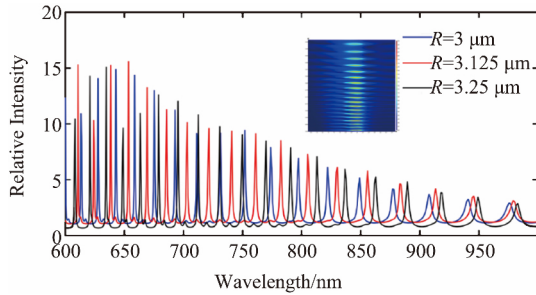
Fig. 7　Relative intensity spectra inside microsphere
图 7

Fig. 8　Experimental schematic diagram（a）the experimen-
tal detection system for the coupling system　（b）experimen-
tal graphs of the silica microsphere coupling system　side
view　and vertical view　（c）typical resonant dip
图 8　　　　　　　　（a）　　　　　　　　　　　（b）
　　　　　　　　　　　（c）

cated by fusing the tip of a single mode fiber（SMF-28）
using a CO_2 laser. When optical fiber absorbs light ener-
gy　the fiber will be melted and form an optical micro-
sphere cavity. The tapered fiber is fabricated by using
the method of heat-and-pull with low insertion loss　in
which the heating source is pure hydrogen flame com-
busted in air. Figure 8（a）presents an experimental de-
tection system for testing their coupling characteristics. A
tunable laser in the 1 550 nm band（New Focus Velocity
6 728　line width < 200 kHz）driven by a 20 Hz triangle-
wave signal generated by the function generator conducts
wavelength scanning. TE and TM mode can be trans-
formed by adjusting the polarization controller. Light
from laser enters the tapered fiber　and then couples into
the microsphere. Photo detector with a 150 MHz band-
width（Thorlabs PDA 10CF-EC）can convert light signal
to electrical signal displayed in the oscilloscope. We ob-
serve the microsphere and tapered fiber with the help of
two charge-coupled device（CCD）cameras. Figure 8
（b）indicates the experimental graphs of the microsphere
coupling system　side view　and vertical view. The radi-
us of the microsphere is about 180 μm and the diameter
of tapered fiber is 2. 5 μm　approximately. Figure 8（c）
depicts a typical WGM resonant dip. The Q factor of sili-
ca-microsphere is calculated by using the line width $Q = \lambda / \Delta\lambda$　where λ and $\Delta\lambda$ stand for the resonance wave-
length and the FWHM of the resonance dip [6]. In our
testing system　a polarization controller is utilized to ad-
just to TM polarized resonance mode and the input power
to the tapered fiber is 0. 1 mW for the purpose of reduc-
ing the thermal effect.

As is shown in Fig. 9（a）　the shape of transmis-
sion spectra shows a good fit to our simulation results.
Likewise　the gap between the microsphere and tapered
fiber can be controlled precisely to improve the coupling
efficiency. Under the condition of the contact between
the microsphere and taper in our experiment　we find
that a high Q up to 2. 3×10^6 of the microsphere-taper
system by adjusting the microsphere orientation carefully
a strong critically-coupling（92. 5%）as a consequence
of phase matching of the fundamental mode to the micro-
sphere WGM. In order to better demonstrate the Q fac-
tors and coupling efficiency of the observed resonant
dips　magnified views of the transmission spectra over
narrow wavelength ranges are presented　as shown in
Fig. 9（b）　which shows a series of typical spectrum
（f1）~（f6）in Fig. 9（a）.（f2）and（f5）are the reso-
nant mode with the highest Q　but a low coupling effi-
ciency due to the under-coupling condition. In addition
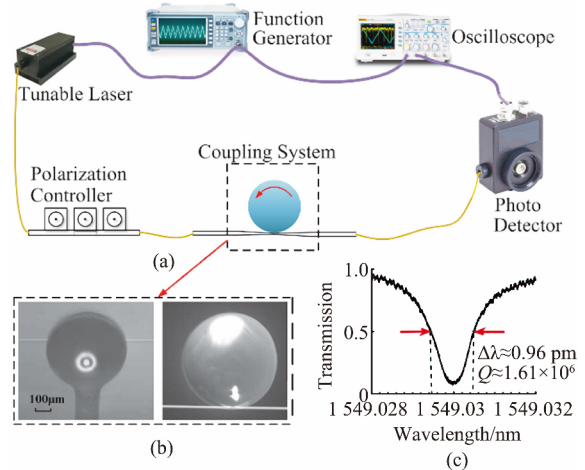
most of the resonant dips　such as（f3）and（f6）　have
a high coupling efficiency thanks to the critically-coupled
condition. Moreover　it can be seen that（f1）　（f4）are
the partial spectral overlap of modes with different azi-
muthal mode numbers. This may result in a lower Q and
another possible reason for the increased WGM losses of
the excited higher-order azimuthal modes. These modes
extend further away from the optical equator　so that they
interact more strongly with the surface imperfections and
the attached fiber stem　giving rise to the Q factor degra-
dation. While testing experiments benefit from a small
mode volume　a large volume　however　may be more
preferable in the field of microcavity-based group delay
lines. Also　a large mode volume resonator is very help-
ful in improving the efficiency and output power of the
WGM microresonator laser.

4　Discussion

From the details of previous sections　we can con-
clude that numerical results present a good fit to our ex-
perimental results. The coupling characteristics can be
explained by our theoretical results. There are several
similarities in our simulation and experiment as summa-
rized below:（1）the transmission spectra distributed as
different wavelengths of continuous wave. Clean resonant
dips all form a peak on their transmission spectra.（2）
the gap between the microsphere and waveguide strongly
affects the coupling efficiency. High coupling efficiency
（>90%）can be realized. We confirmed that the cou-
pling characteristics of the microsphere cavity coupled by
a waveguide can be optimized by controlling phase-matc-
hing.

Moreover　Q factors are a direct measure of the abil-
ity of the cavity to confine and store light. Q factor is one
of coupling characteristics and one of the most important
properties of optical resonances in any kind of geomet-
rical resonator. The overall Q factor is explicitly defined

3

WANG Meng-Yu *et al*: Analysis for coupling characteristics of optical microsphere cavity in
waveguide coupled whispering gallery mode

289
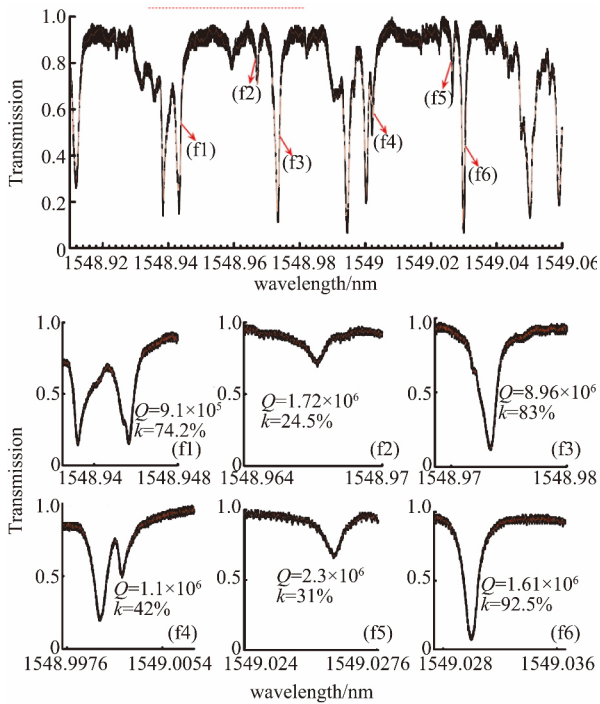
Fig. 9　Transmission spectra of experimental result（a）transmission spectrum of the coupling system over a wavelength range of 1 558. 915 ~ 1 549. 06 nm；（b）（f1）~（f6）typical transmission spectra of the coupling system for the microsphere
9　　　　　　　　（a）　　　　　1 558. 915 ~
1 549. 06 nm　　　　　　　（b）
（f1）~（f6）

Fig. 10　The calculation of Q factor （a）the biggest Q factor in the simulation （b）the biggest Q factor in the experiment （c）the time signal for the resonant wavelength 663. 251 nm in the simulation （d）the log of the time signal envelope

10　　　　　　　　Q　（a）　　　　　　　Q　（b）
　　　　　　　Q　（c）　　　　　　　663. 251
nm　　　　　　（d）

by the following equation [7] as $Q_{tot}^{-1} = Q_{in}^{-1} + Q_{ext}^{-1}$ corresponding to an overall photon lifetime τ_{ph} and resonance linewidth $Q_{tot} = w_o \tau_{ph}$ w_0 is the resonant frequency of the WGM. The intra-cavity losses are characterized by the intrinsic Q factor $Q_{in}^{-1} = Q_{mat}^{-1} + Q_{rad}^{-1} + Q_{sur}^{-1}$ in order to consider the intra-cavity volumic losses （Q_{mat}） radiation losses （Q_{rad}） surface scattering roughness （Q_{sur}） respectively. Q_{rad} is relevant to the size of the cavity. The coupling （or external）Q factor is Q_{ext} which depends on the performance of the coupling using the waveguide （or the tapered fiber）. We can calculate Q_{tot} factors by getting FWHM of resonant dips in our simulation and experiment. The highest Q factor can be obtained after processing these data as shown in Figs. 10（a）and（b）. We find resonant dip will have the highest Q factor when resonance is in the critically-coupling condition （$Q_{in} < Q_{ext}$） both numerically and experimentally. However compared to Q factors in our experiment （$10^5 ~ 10^6$） the simulation method predicts a lower Q factor （$10^2 ~ 10^3$）. In fact the FDTD simulation time step Δt is too small compared to the real situation. Small Δt is the main reason for the Q factor difference. Mathematically a microsphere cavity is considered to be a high-Q resonator when the EM fields cannot completely decay from the simulation in a time that can be simulated reasonably by FDTD.

In addition a smaller microsphere （$R = 3. 25$ μm）is another reason limited by the meshed gird （600

× 600）. We cannot reduce calculation accuracy to calculate a bigger microsphere so that Q_{rad} in the simulation is smaller than Q_{rad} in the experiment. The simulation time is too long and the required memory is too much. In our work we cannot determine a high Q factor from the FWHM as shown Fig. 10（a）based on simulation time. Instead Q factors can be determined by the slope of the envelope of the decaying signal [8] using the formula: $Q = -w_0 \log_{10} e/2m$ m is the slope of the log of the time signal envelope as shown in Fig. 10（c）. As shown in Fig. 10（d） we can calculate the Q factor: $Q = 5 238. 44 \approx 5. 24 \times 10^3$. The result is much closer to the real experiment result but there is still a big difference. The biggest Q factor in the experiment is almost 400 times higher than that by calculating the FWHM and 1 000 times higher than that by calculating the slope of the log of the time signal envelope.

5　Conclusions

In summary coupling characteristics in a waveguide to a silica-microsphere system are studied numerically and experimentally. We have observed the coupling structures that a smaller volume microsphere （$R = 3. 25$ μm）coupling by a waveguide using a 2D model in our simulation and a bigger volume microsphere （$R = 180$ μm） fabricated by melting the tip of a single fiber with CO_2 laser couples with a tapered fiber in our experiment. In our simulation the coupling efficiency increases remarkably with a decrease of the gap from 130 nm to
（　　　337　　）

liquely on a narrowband filter ［J］. *Acta Photonica Sinica* （ . ） 2010 **39**（11）: 1971-1975.

12 Qian L Zhang D Huang Y *et al*. Performance of a double-layer guided mode resonance filter with non-sub-wavelength grating period at oblique incidence ［J］. *Optics & Laser Technology*. 2015 **72**: 42-47.

13 Ciminelli C Peluso F Armenise M N *et al*. Variable oblique incidence for tunability in a two-dimensional photonic-crystal guided-wave filter ［J］. *Journal of Lightwave Technology*. 2006 **24**（1）: 470-476.

14 YU Kan LIU Wen HUANG De-Xiu. Characteristics analysis and stack design of angle-tuned filter ［J］. *Acta Photonica Sinica*（ . ） 2008 **37**（6）: 1175-1179.

15 Mcleod R R Honda T. Improving the spectral resolution of wedged etalons and linear variable filters with incidence angle ［J］. *Opt Lett*. 2005 **30**（19）: 2647-2649.

16 CAO Jian-Zhang. Thin film optical and thin film technology foundation ［M］. Beijing: Science Press（ . : ） 2014.

17 Shaowei W Xiaoshuang C Wei L. Fabrication of Step Filter for Miniature Wavelength-Division Device Based on Photolithography ［J］. *Acta Optica Sinica*. 2009 **29**（5）: 1358-1362.

18 LIN Bing YU Tian-Yan LI Da-Qi *et al*. Study of fabrication of 16-channel micro integrated filter ［J］. *J. Infrared Millim. Waves*（ . 16 . ） 2006 **25**（04）: 287-290.

19 LU Jin-Jun. Optical film technology ［M］. Xian: Press of Northwestern Polytechnical University（ . . ） 2005.

20 Zhang Y G Zhuang X G Wang X Q *et al*. Wavelength calibration of a new monolithically integrated spectral sensor ［J］. *Journal of Infrared & Millimeter Waves*. 2017 **36**（01）: 15-19.

10 nm. In our experiment Q factor （2.3×10^{6}） and strong critically-coupling （92.5%） as a consequence of phase matching were reached. We confirmed that exceedingly efficient and controlled power transfer from a waveguide to a high Q microsphere is possible. We believe that the results will open the way for new applications in some fields such as bio-sensors and micro-lasers.

Acknowledgment

References

1 Heebner J Grover R Ibrahim T. Optical Microresonators ［J］. *Optical Sciences* 2008 **138**: 71-103.

2 Panitchob Y Murugan G S Zervas M N *et al*. Whispering gallery mode spectra of channel waveguide coupled microspheres ［J］. *Optics Express* 2008 **16**（15）: 11066-11076.

3 Hall J M Shahraam A V Henderson M R *et al*. Method for predicting whispering gallery mode spectra of spherical microresonators ［J］. *Optics Express* 2015 **23**（8）: 9924-9932.

4 Chiasera A Dumeige Y Féron P *et al*. Spherical whispering-gallery mode microresonators ［J］. *Laser & Photonics Review* 2010 **4**（3）: 457-482.

5 Dominguez J L Kozyreff G Jordi M. Whispering gallery microresonators for second harmonic light generation from a low number of small molecules ［J］. *Nature Communications* 2011 **2**（1）: 254.

6 Elliott G R Murugan G S Wilkinson J S *et al*. Chalcogenide glass microsphere laser ［J］. *Optics Express* 2010 **18**（25）: 26720-26727.

7 Murugan G S Wilkinson J S Zervas M N *et al*. Integrated Nd-doped borosilicate glass microsphere laser ［J］. *Optics letters* 2011 **36**（1）: 73-75.

8 Athanasiou M Smith R M Pugh J *et al*. Monolithically multi-color lasing from an InGaN microdisk on a Si substrate ［J］. *Scientific Reports* 2017 **7**（1）: 10086.